ACS OMEGA

http://pubs.acs.org/journal/acsodf

Article

Hydrochloride Salt of the GABAkine KRM-II-81

Md Yeunus Mian,* Branka Divović, Dishary Sharmin, Kamal P. Pandey, Lalit K. Golani, V. V. N. Phani Babu Tiruveedhula, Rok Cerne, Jodi L. Smith, Xingjie Ping, Xiaoming Jin, Gregory H. Imler, Jeffrey R. Deschamps, Arnold Lippa, James M. Cook, Miroslav M. Savić, James Rowlett, and Jeffrey M. Witkin

Cite This: *ACS Omega* 2022, 7, 27550−27559

Read Online

ACCESS | Metrics & More | Article Recommendations | Supporting Information

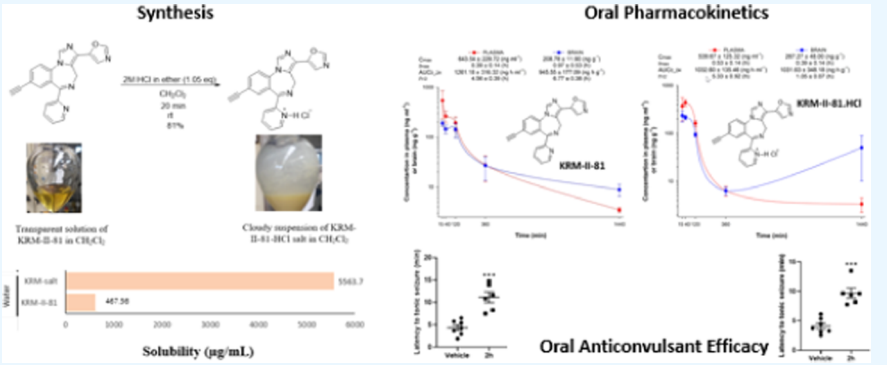

ABSTRACT: Imidazodiazepine (5-(8-ethynyl-6-(pyridin-2-yl)-4*H*-benzo[*f*]imidazole[1,5-*α*][1,4]diazepin-3-yl) oxazole or KRM-II-81) is a potentiator of $GABA_A$ receptors (a GABAkine) undergoing preparation for clinical development. KRM-II-81 is active against many seizure and pain models in rodents, where it exhibits improved pharmacological properties over standard-of-care agents. Since salts can be utilized to create opportunities for increased solubility, enhanced absorption, and distribution, as well as for efficient methods of bulk synthesis, a hydrochloride salt of KRM-II-81 was prepared. KRM-II-81·HCl was produced from the free base with anhydrous hydrochloric acid. The formation of the monohydrochloride salt was confirmed by X-ray crystallography, as well as ^{1}H NMR and ^{13}C NMR analyses. High water solubility and a lower partition coefficient (octanol/water) were exhibited by KRM-II-81·HCl as compared to the free base. Oral administration of either KRM-II-81·HCl or the free base resulted in high concentrations in the brain and plasma of rats. Oral dosing in mice significantly increased the latency to both clonic and tonic convulsions and decreased pentylenetetrazol-induced lethality. The increased water solubility of the HCl salt enables intravenous dosing and the potential for higher concentration formulations compared with the free base without impacting anticonvulsant potency. Thus, KRM-II-81·HCl adds an important new compound to facilitate the development of these imidazodiazepines for clinical evaluation.

INTRODUCTION

KRM-II-81 is the latest in a series of imidazodiazepine potentiators of $GABA_A$ receptors (GABAARs) or GABAkines that is under development.[1,2] KRM-II-81 produces anxiolytic effects,[3,4] antidepressant-like activity,[5] anticonvulsant activity,[6−9] and efficacy in a host of acute and chronic pain models in rodents.[10] The efficacy of KRM-II-81 is associated with a low sedative and motor-impairing profile, lack of tolerance development, and abuse liability.[2,10] Further, KRM-II-81 is efficacious in models of pharmacoresistant epilepsy[7] and did not produce tolerance.[7,11] In animal models used to predict drug abuse liability, KRM-II-81 differentiated from classical GABAkines like midazolam or diazepam.[2]

Salt formation has been considered as an important step during the preformulation stage of drug development.[12,13] Preparing a salt form can overcome the nonoptimal physicochemical and/or biopharmaceutical properties of an ionizable molecule.[14] The key salt form selection early in the development process can improve the bioavailability of a compound. Proper salt form selection is facilitated by an efficient salt screening strategy that involves the evaluation of crystallinity, hygroscopicity, solubility, stability, purity, polymorphism/hydrate formation, and powder flowability, in addition to the practical importance of cost and reaction

Received: May 15, 2022
Accepted: July 14, 2022
Published: July 27, 2022

yield.[15,16] In addition to enhancing physiochemical and biopharmaceutical properties of compounds,[17] creation of salts has also been shown to improve compound druggability.[18]

Here, the preparation and characterization of a HCl salt of KRM-II-81 are reported (Figure 1). HCl was chosen as the first

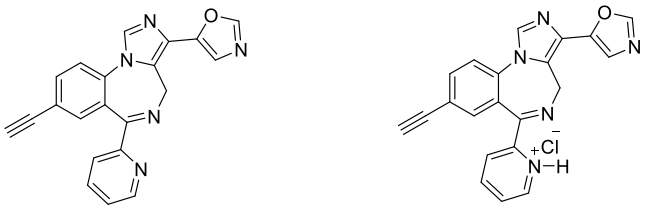

Molecular Weight: 351.37
KRM-II-81

Molecular Weight: 387.83
KRM-II-81·HCl

Figure 1. Structures of KRM-II-81 and the HCl salt reported here.

salt to construct because the chloride counterion from HCl provides better solubility than the counterions from phosphoric acid, malonic acid, maleic acid, and fumaric acid, and we did not consider formic acid as this is not under the salt approval category by the FDA.[18] The physiochemical properties of the KRM-II-81·HCl salt will be described along with in vivo studies of plasma and brain exposure after oral administration. Comparative anticonvulsant potency and efficacy of KRM-II-81·HCl relative to the free base will also be described.

RESULTS AND DISCUSSION

Synthesis. To prepare KRM-II-81·HCl, one needs to synthesize KRM-II-81 as a precursor. An improved, scalable synthetic method for KRM-II-81 was developed by Knutson et al.[9] KRM-II-81 was synthesized according to that procedure. Then, an optimized method was developed for preparing the KRM-II-81·HCl salt. This is a simple, robust, and easily handled process. The synthetic method is depicted in Scheme 1.

KRM-II-81 was dissolved in anhydrous dichloromethane after stirring for a period of about 20 min. When heat (30−35 °C) was applied to the mixture, a clear solution was obtained. The dropwise addition of anhydrous HCl (2 M solution in ether) to the reaction with stirring resulted in a cloudy suspension, which indicated the formation of the salt. Simple filtration and washing with anhydrous dichloromethane afforded the pure HCl salt. The product obtained was characterized by NMR spectroscopy and X-ray crystallography.

Analysis of the KRM-II-81·HCl Salt with ^{1}H NMR and ^{13}C NMR Spectroscopy. The protonation of the tertiary nitrogen atom in KRM-II-81 effects a downfield shift of the hydrogen atoms present on the adjacent carbon atoms in the ^{1}H NMR spectrum. The cation in the spectrum of the KRM-II-81·HCl salt showed a downfield shift in δ ppm values of the hydrogen atoms of the pyridine ring, which was expected. The protons near the nitrogen atom showed chemical shift differences in the ^{1}H NMR spectrum of KRM-II-81 (the free base) and its HCl salt (Figure 2a). A notable difference in chemical shift values was observed between the hydrogen atoms at C-16 and C-13 near the pyridine nitrogen atom of the free base and the salt. The chemical shift value of the proton at C-16 was 8.5 ppm, which was shifted downfield by 0.17 ppm (to 8.67 ppm) in the HCl salt of KRM-II-81. The proton at C-13 of the pyridine ring appeared at 8.47 ppm in the free base; however, it was shifted downfield in the HCl salt to 8.60 ppm. Another proton (proton 15) of the 2′-pyridine ring was also shifted downfield by 0.14 ppm in the HCl salt. It appeared at 7.48 ppm in the free base, whereas this was found at 7.62 ppm in the salt. Minor shifts were observed in the case of proton 14. Interestingly, protons at C-26 and at C-24 of the oxazole ring were also shifted downfield by 0.1 ppm and 0.07 ppm, respectively. The proton at C-26 was shifted from 7.44 ppm (free base) to 7.54 ppm (HCl salt), whereas proton 24 appeared at 7.51 ppm in the salt. Proton H9′, one of the diastereotopic protons, was also shifted downfield by 0.08 ppm (4.36−4.44 ppm). The perturbations observed in the ^{1}H chemical shifts for the HCl salt of KRM-II-81 are shown in Figure 2b. The chemical shift differences were also observed in the ^{13}C NMR spectrum of the free base and its salt (see the Supporting Information).

Single-Crystal X-ray Diffraction Analysis of KRM-II·HCl. To verify the monohydrochloride position in the KRM-II-81 hydrochloride salt and correlate it to the NMR studies, single-crystal X-ray analysis was carried out, and a representation of the structure is illustrated in Figure 3. The tables of bond angles, bond lengths, and electron densities, as well as the discussion of the NMR spectrum, are given in the Supporting Information. The NMR chemical shifts are important because they will be useful for correlations when other salts of KRM-II-81 are prepared. The single-crystal X-ray diffraction analysis of KRM-

Scheme 1. Synthesis of KRM-II-81·HCl (Photograph Courtesy of Md Yeunus Mian, Copyright 2022)

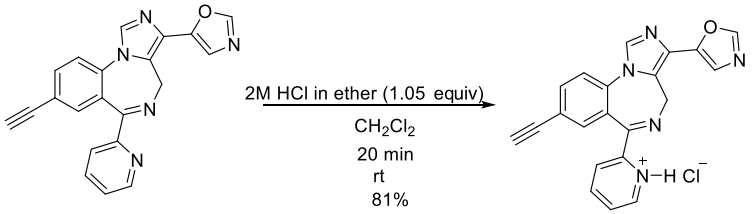

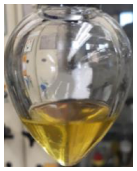

Transparent solution of KRM-II-81 in CH_2Cl_2

Cloudy suspension of KRM-II-81-HCl salt in CH_2Cl_2

https://doi.org/10.1021/acsomega.2c03029
ACS Omega 2022, 7, 27550−27559

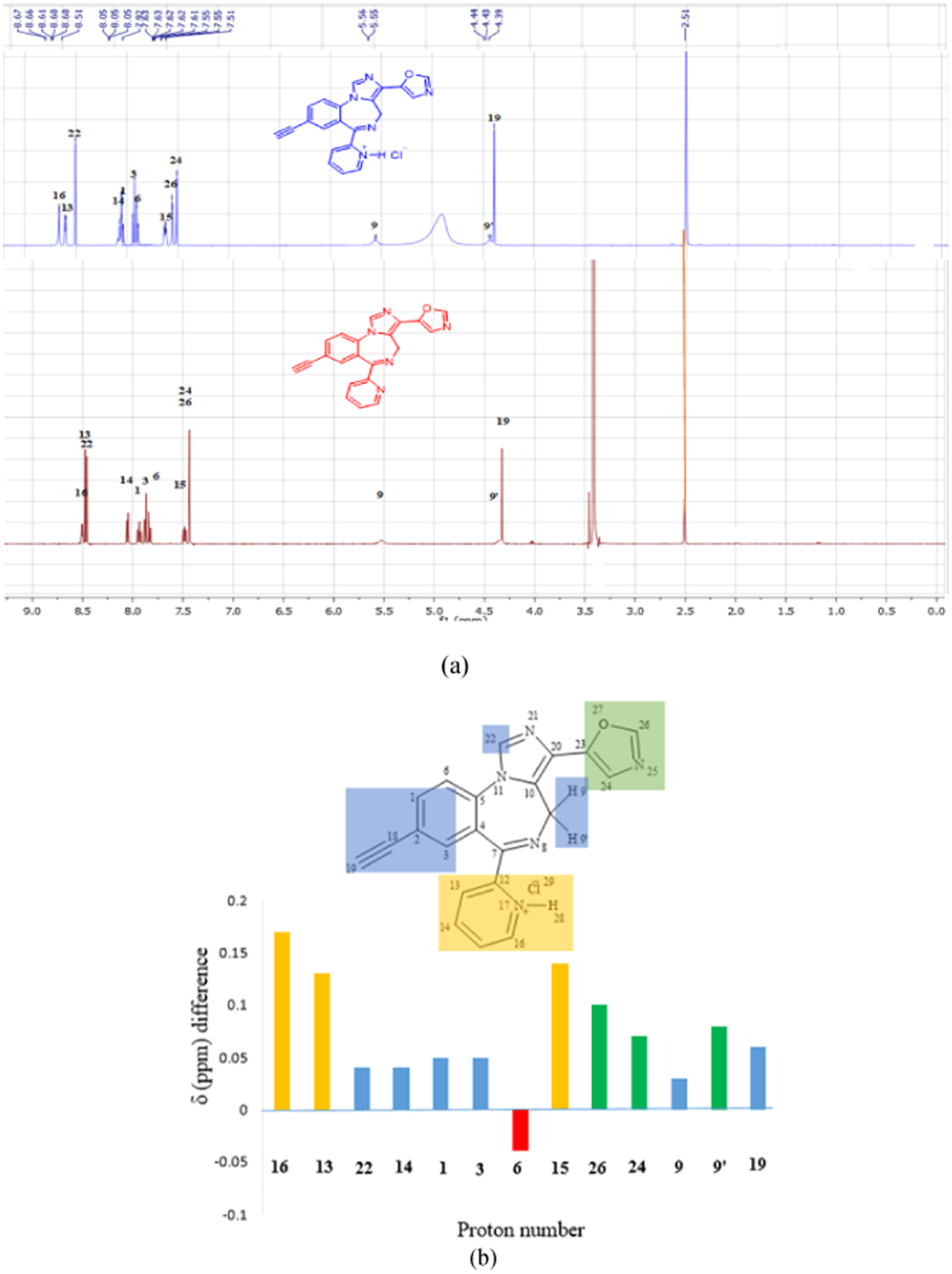

Figure 2. (a) ^{1}H NMR spectrum overlay of KRM-II-81 and its HCl salt (in DMSO-d_6). (b) ^{1}H chemical shift differences of the KRM-II-81·HCl salt.

II-81·HCl revealed that only the monochloride salt formed, and the salt formation occurred on the 2′-pyridine nitrogen atom, as desired.

Physical Characterization. Solubility and Partition Coefficient of the KRM-II-81·HCl Salt. Preformulation parameters such as solubility, partition coefficient (log *P*), and hygroscopicity are highly important during the design of a dosage form

https://doi.org/10.1021/acsomega.2c03029
ACS Omega 2022, 7, 27550−27559

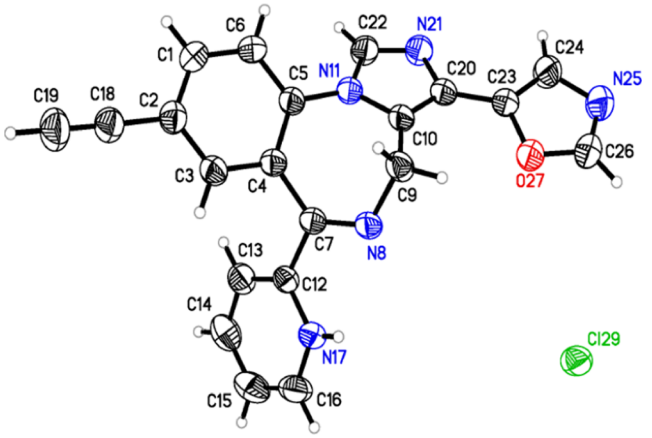

Figure 3. Model of KRM-II-81·HCl based on X-ray diffraction studies. Examination of the X-ray crystal structure confirmed the formation of the monohydrochloride salt, and it formed on the pyridine nitrogen. This is a thermal ellipsoid plot of KRM-II-81·HCl with thermal ellipsoids drawn at the 50% probability level.

of drugs. These parameters directly influence the absorption of orally administered drugs. Particle size reduction, nanosuspension, use of surfactants, salt formation, solid dispersion, etc. represent several techniques used to enhance compound solubility.[19] The solubility and dissolution rates of acidic and basic drugs can be increased by forming a salt form of the corresponding drug.

The solubility of the hydrochloride salt of KRM-II-81 and its free base was determined in a number of solvents (Figure 4). KRM-II-81·HCl showed high water solubility when compared to the free base (467.5 ± 1 μg/mL). The thermodynamic equilibrium solubility value of the KRM-II-81·HCl salt was 5563 ± 15 μg/mL. Approximately 13-fold improvement in water solubility was observed for the salt form in comparison to that for the free base. The solubility of the KRM-II-81·HCl salt and the free base in water was also determined manually. The result was that the KRM-II-81·HCl salt was 14 times more soluble in water than its free base. The water solubility data were completely consistent with the solubility data from the spectroscopic method.

The partition coefficient is a parameter by which the hydrophilicity/lipophilicity of a compound can be measured. This parameter is considered as one of the important characteristics of any potential drug because it determines to a large extent a drug candidate's fate both inside a living organism and in the environment.[20] It plays an important role in the preformulation study of a drug molecule. The log *P* of KRM-II-81·HCl was determined, and the value for the salt was 0.53 ± 0.06, indicating the hydrophilic nature of the salt over the free base (log *P* = 1.763 ± 0.12). The log *P* value is in agreement with the solubility data; salt formation increases the water solubility and decreases the lipophilicity, as expected.

Solubility of the KRM-II-81·HCl Salt at Different pH Values. The aqueous solubility of the KRM-II-81·HCl salt was determined at different pH values by the shake-flask method using UV absorbance measurements at 300 nm (Figure 5).

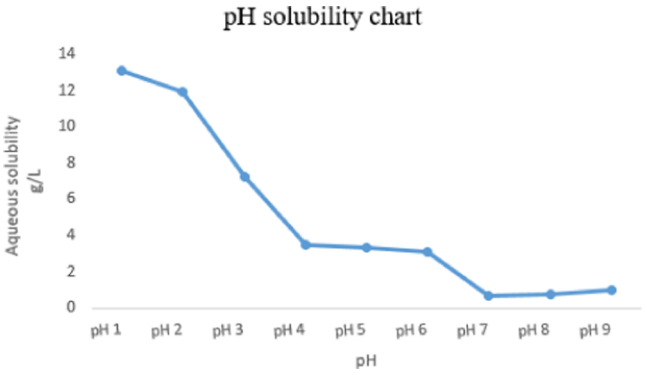

Figure 5. Solubility of the KRM-II-81·HCl salt at different pH values in water determined after 24 h in a shake flask using UV absorption at 300 nm.

Excellent solubility of KRM-II-81·HCl was observed at a lower pH (1, 2, and 3 in g/L), whereas lower solubility was observed at a neutral pH. Aqueous solubility decreased as the pH increased. The highest solubility of the KRM-II-81·HCl salt was observed at pH 1 (13.1 g/L). The lowest solubility was observed at pH 7 (5.4 g/L), whereas the solubility was slightly increased at pH 8 and 9. This pH−solubility behavior of KRM-II-81·HCl was similar to that of midazolam, which shows more solubility at a

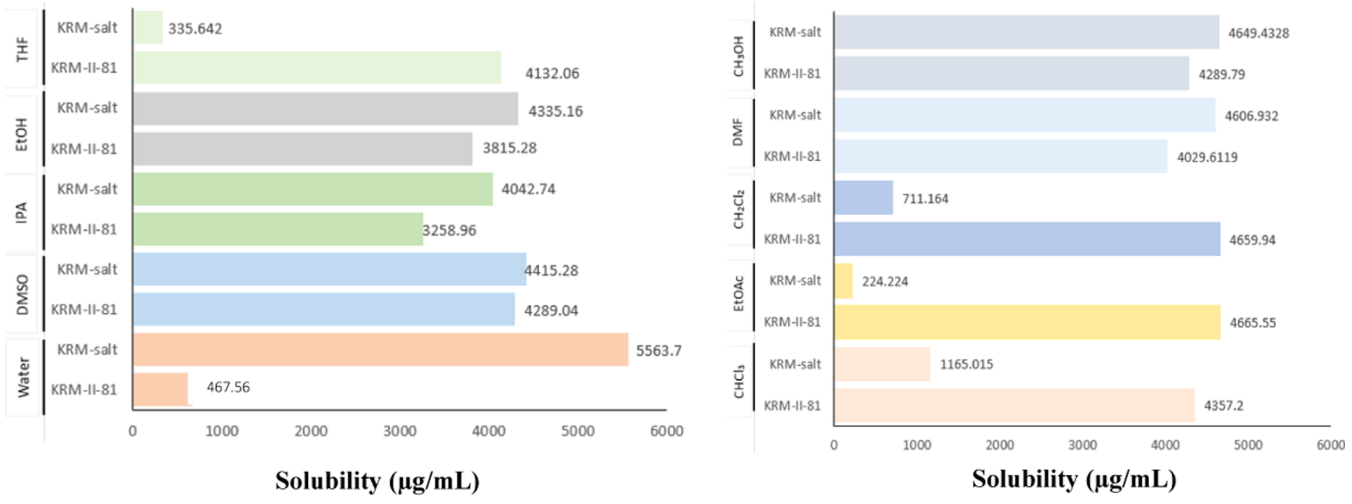

Figure 4. Solubility of KRM-II-81 and its HCl salt in water and other solvents. Different colors represent the solubility in different solvents.

https://doi.org/10.1021/acsomega.2c03029
ACS Omega 2022, 7, 27550−27559

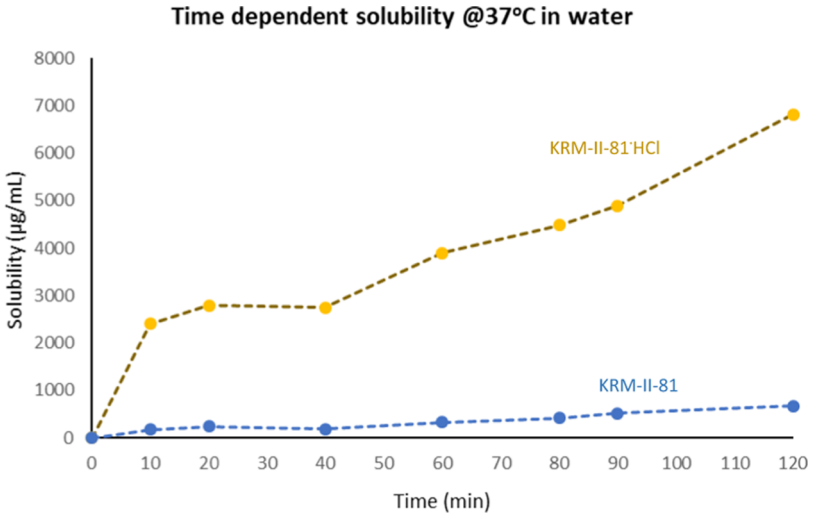

Figure 6. Kinetic solubility of KRM-II-81 and its HCl salt at 37 °C in water. The blue line represents the time-dependent solubility of KRM-II-81, and the orange line represents the time-dependent solubility of KRM-II-81·HCl.

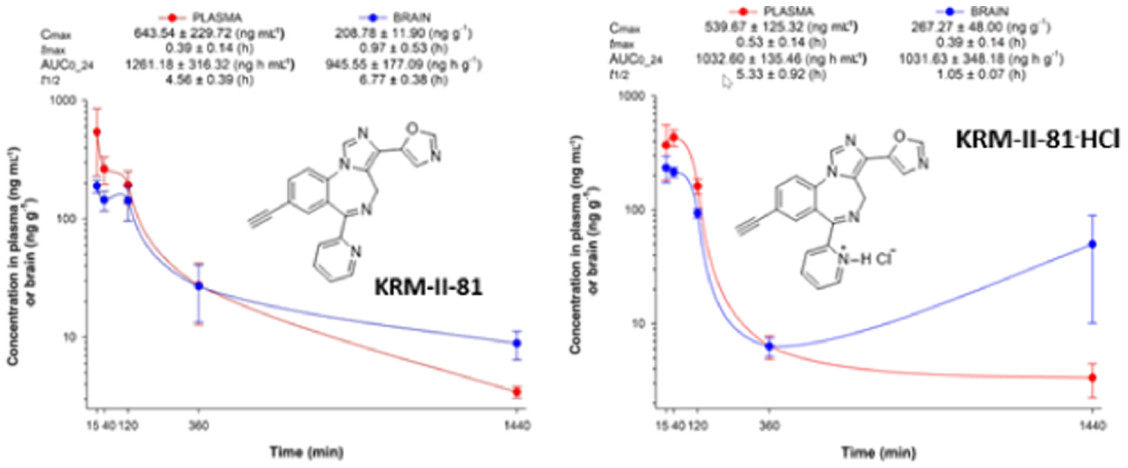

Figure 7. Pharmacokinetics of KRM-II-81 and KRM-II-81·HCl in the plasma and brain after oral administration of 2.0 mg/kg in rats. Each point represents the mean ± standard error of the mean (SEM) in three rats.

lower pH, but it is less soluble at a neutral pH (70 mg/L) due to the protonation of imidazole nitrogen atoms,[21] as expected.

Hygroscopicity of KRM-II-81·HCl. The hygroscopicity of a compound is the capacity to absorb atmospheric moisture. The amount of moisture absorbed depends on atmospheric conditions along with the crystal stability and surface area of the material. Any changes in the moisture level of a drug can impact its chemical stability, flowability, and compressibility, and this is the main reason for determining the hygroscopicity of KRM-II-81·HCl. The hygroscopicity of KRM-II-81·HCl was determined and found to be only slightly hygroscopic. According to the European Pharmacopoeia, there are four different classes of hygroscopicity: Class I, nonhygroscopic (<0.2%, w/w); Class II, slightly hygroscopic (0.2−2%, w/w); Class III, hygroscopic (2−15%, w/w); and Class IV, very hygroscopic (>15%, w/w). The increase in weight for KRM-II-81·HCl was 0.18% w/w, which falls under the category Class I. Weight changes on simply storing the KRM-II-81·HCl salt exposed to air were nil (<0.2%). The low hygroscopic property of KRM-II-81·HCl will help to minimize the risk associated with moisture during preformulation and storage.

Kinetic Solubility Assessment. Increasing drug solubility while maintaining a stable form is one of the important aspects of solid-state pharmaceutical development. This is challenging because of the two major factors that are used to describe oral absorption: one of them is solubility and the other one is permeability. To find out the extent of the supersaturation state of KRM-II-81 and its HCl salt in water, the time-dependent solubility of both of the compounds was determined at 37 °C in water (Figure 6).

The HCl salt of KRM-II-81 was found to remain in the solution state for a longer period of time in comparison with the free base, KRM-II-81. The KRM-II-81·HCl salt was able to inhibit its crystallization for a prolonged period of time. High apparent solubility was observed due to the sustained parachute effect. The high apparent solubility of the compound reasonably could improve absorption and distribution in vivo.

Oral Dose Pharmacokinetics. A pharmacokinetic study was performed to evaluate the in vivo fate, after oral gavage in rats, of KRM-II-81, as compared to its HCl salt. Kinetic profiles of plasma and brain exposure for both compounds are shown in Figure 7. The plasma and brain exposed to the compounds exhibited the highest concentrations of compound initially than

https://doi.org/10.1021/acsomega.2c03029
ACS Omega 2022, 7, 27550−27559

Table 1. Concentrations of Compounds in the Plasma and Brains of Rats after Oral Dosing (2 mg/kg) and the Brain-to-Plasma Ratios Derived from These Values[a]

compound	C_{max} (plasma)	C_{max} (brain)	C_{max} (brain/plasma)	AUC 24 h (plasma)	AUC 24 h (brain)	AUC 24 h (brain/plasma)
KRM-II-81	1831.5	594.2	0.32	3589.3	2689.5	0.77
KRM-II-81·HCl	1319.5	689.1	0.52	2662.5	2660.0	1.00

[a]Concentrations are in nM.

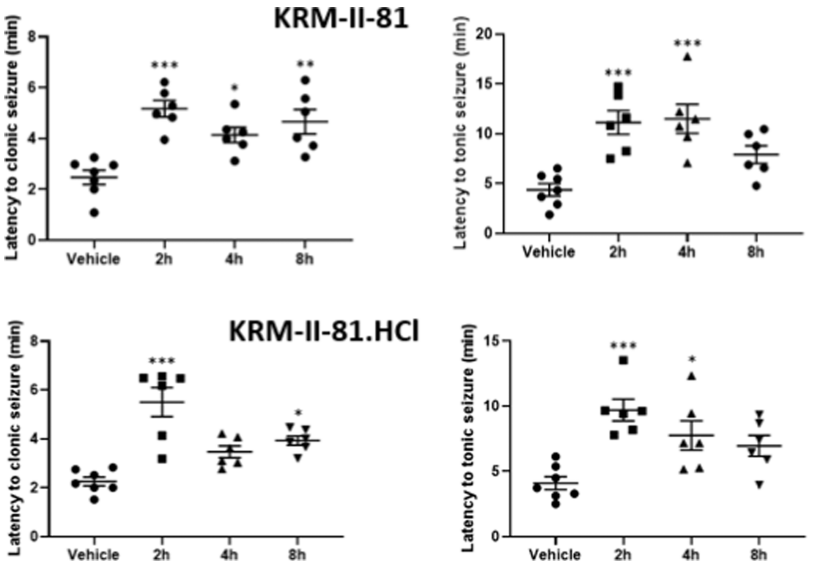

Figure 8. Effects of orally administered KRM-II-81 (top panels) and KRM-II-81·HCl (bottom panels) (10 mg/kg) on the latency to produce clonic (left panels) or tonic (right panels) seizures after 70 mg/kg pentylenetetrazol in mice. *, **, and ***: $P < 0.05$, 0.01, and 0.001 compared to respective vehicle control value. $N = 6–7$ mice per group.

later after oral dosing. However, at 24 h after dosing with KRM-II-81·HCl, the brain levels showed an increasing trend above the levels observed at 6 h.

Using the compound concentration summary parameters of C_{max} and area under the curve (AUC) (Table 1), it can be seen that the plasma levels achieved by these two compounds were both high (>1 μM) and generally comparable to one another. Brain levels too were high, with C_{max} levels that exceeded 0.5 μM. The brain-to-plasma ratio for the two compounds differed, with KRM-II-81·HCl achieving higher brain/plasma levels than the free base, but this difference did not achieve statistical significance (Figure 8).

Oral Dosing: Pentylenetetrazole (PTZ) Seizures. Both KRM-II-81 and KRM-II-81·HCl demonstrated anticonvulsant activity against pentylenetetrazol-induced clonic and tonic convulsions in mice after oral administration of 10 mg/kg (Figure 7). Both the base and the HCl salt of KRM-II-81 generally exhibited comparable effects with approximately a doubling of the latency to produce convulsions from 2 to 8 h after oral dosing. The peak time of efficacy was about 2 h.

In addition to producing convulsions in mice, 70 mg/kg pentylenetetrazol also produced lethality in 57.1% of mice tested (Table 2). The prevalence of lethality was reduced by both compounds at all timepoints post dosing (trend for effect for KRM-II-81·HCl at the last two timepoints).

Conclusions. The HCl salt of KRM-II-81 can be easily synthesized from the free base. The solubility of KRM-II-81 is 13× that of the free base in water. Solubility enhancements of this type will enable future in vivo studies that require intravenous dosing (drug self-administration in drug abuse liability studies) as well as increased drug concentrations that can be prepared. Although the HCl did not improve the pharmacokinetics of the free base after oral administration, KRM-II-81·HCl retained the ability to achieve high plasma and brain levels of drug when given in a water formulation. The HCl salt was also efficacious as an anticonvulsant, which bodes well for its future use in the drug development process toward antiepileptic drug use. Importantly, the data from the present study take the first steps in salt selections for the ongoing development of KRM-II-81 for the clinic.

Table 2. Reduction of Pentylenetetrazol (70 mg/kg) Produced Lethality by KRM-II-81 and Its HCl Salt

compound	lethality/number tested	latency to death (s)
vehicle	4/7	25.75 ± 8.02
KRM-II-81 (2 h)	0/6[a]	
KRM-II-81 (4 h)	0/6[a]	
KRM-II-81 (8 h)	0/6[a]	
KRM-II-81·HCl (2 h)	0/6[a]	
KRM-II-81·HCl (4 h)	1/6	15.68
KRM-II-81·HCl (8 h)	1/6	43.00

[a]$P < 0.05$.

MATERIALS AND METHODS

Chemistry. *General Procedure for the Synthesis of the KRM-II-81 Hydrochloride Salt.* The reaction was performed in a conical-shaped flask with a magnetic stir bar under an argon atmosphere. Organic solvents and chemicals were purified when necessary by standard methods or purchased from either Sigma-Aldrich, Admiral Chemical Company, or Acros Organic. The ^{1}H

https://doi.org/10.1021/acsomega.2c03029
ACS Omega 2022, 7, 27550−27559

and ^{13}C NMR data were obtained on a Bruker Avance III 500 MHz spectrometer with chemical shifts in δ (ppm).

Synthesis of 2-(8-Ethynyl-3-(oxazol-5-yl)-4H-benzo[f]-imidazo[1,5-a][1,4]diazepin-6-yl)pyridin-1-ium Chloride (MYM-V-26, KRM-II-81·HCl). 5-(8-Ethynyl-6-(pyridin-2-yl)-4*H*-benzo[*f*]imidazo[1,5-*a*][1,4]diazepin-3-yl)oxazole (KRM-II-81, 0.5 g, 1.42 mmol) was dissolved in anhydrous dichloromethane (8 mL) under an argon atmosphere at 30−35 °C. The light-yellow clear solution obtained was then cooled down to room temperature and a 2 M solution of anhydrous HCl in ether (0.75 mL, 1.49 mmol) was added dropwise to the reaction mixture over a period of 10 min. A light-yellow cloudy suspension resulted during the addition of HCl. The reaction mixture was then stirred for 30 min until the consumption of starting material. The consumption of starting material was confirmed by thin-layer chromatography (TLC). The precipitate from the reaction mixture was filtered and washed with anhydrous dichloromethane (2 × 8 mL) to remove any unreacted starting material. The residue was then dried under vacuum at 30−35 °C to afford a light-yellow color amorphous solid, KRM-II-81·HCl salt (0.457 g, 83% yield).

^{1}H NMR and ^{13}C NMR Analyses. The ^{1}H spectra of the KRM-II-81·HCl salt were recorded on a Bruker Avance III 500 MHz spectrometer using deuterated dimethyl sulfoxide (DMSO-d_6). ^{13}C NMR spectra were recorded at 126 MHz. Four milligrams of salt was placed in an NMR tube, and 500 μL of DMSO-d_6 was added to the tube. The NMR tube was shaken vigorously to dissolve the material, followed by ^{1}H NMR and ^{13}C NMR measurements.

2-(8-Ethynyl-3-(oxazol-5-yl)-4H-benzo[f]imidazo[1,5-a]-[1,4]diazepin-6-yl)pyridin-1-ium Chloride (MYM-V-26, KRM-II-81·HCl). ^{1}H NMR (500 MHz, DMSO) δ 8.67 (ddd, J = 4.9, 1.3, 0.8 Hz, 1H), 8.60 (d, J = 4.0 MHz, 1H), 8.51 (s, 1H), 8.09−7.99 (m, 2H), 7.93 (d, J = 8.4 Hz, 1H), 7.89 (dd, J = 8.4, 1.7 Hz, 1H), 7.62 (td, 1H), 7.55 (s, 1H), 7.51 (s, 1H), 5.56 (d, J = 3.4 Hz, 1H), 4.44 (d, J = 7.8 Hz, 1H), 4.39 (s, 1H). ^{13}C NMR (126 MHz, DMSO) δ 167.10 (s), 151.88 (s), 148.12 (s), 148.10 (s), 145.73 (s), 139.19 (s), 137.27 (s), 136.06 (s), 135.76 (s), 135.72 (s), 129.65 (s), 126.47 (s), 126.27 (s), 124.99 (s), 124.33 (s), 122.85 (s), 120.58 (s), 83.26 (s), 82.34 (s), 44.79 (s).

Formation of Crystals. Four milligrams of the KRM-II-81·HCl salt was placed in a 6 mL disposable scintillation vial, and 0.5 mL of anhydrous methanol, 1 mL of anhydrous dichloromethane, and 1 mL of anhydrous hexane were added individually. The flask was shaken at 50 °C and 300 rpm for about 5 min to prepare a clear solution. The contents were then cooled down to room temperature and then kept in the refrigerator overnight. The crystals (clear, colorless, sugarlike) that formed were collected the next morning, dried, and subjected to X-ray diffraction analysis.

Single-Crystal X-ray Diffraction Analysis. A clear colorless block crystal of dimensions 0.147 × 0.048 × 0.030 mm^3 was mounted on a MiTeGen MicroMesh using a small amount of Cargille Immersion Oil. Data were collected on a Bruker three-circle platform diffractometer equipped with a Photon II CPAD detector. The crystals were irradiated using a 1 μS microfocus Mo Kα source (λ = 0.71073) with HELIOS multilayer optics.

The data collection was performed, and the unit cell was initially refined using *APEX3* [v2019.1-0].[22] The data reduction was performed using *SAINT* [v8.38A][23] and *XPREP* [v2014/2].[24] Corrections were applied for Lorentz polarization, and absorption effects were applied using *SADABS* [v2016/2].[25] The structure was solved and refined with the aid of the program SHELXL-2018/3[26] (see the SI for coordinates, etc.).

Physical Characterization. *Determination of Solubility.* The solubility in water and other solvents was determined according to the published procedure.[27] Briefly, 3 mg of KRM-II-81 or the KRM-II-81·HCl salt was added to 200 μL of water or other corresponding solvents in a 1.5 mL microcentrifuge tube, which were mixed using a vortex mixer for 5 min. The samples were further shaken at 300 rpm at 25 °C for 24 h. The mixtures were then transferred to Eppendorf tubes and centrifuged for 5 min at 16 000*g*. The 100 μL of supernatants was transferred to another Eppendorf tube and diluted with methanol. At this point, 50 μL of the diluted samples were then transferred into a 384-well plate (Coring UV star, 781801) for UV detection at 300 nm (Tecan M1000). Triplicate assays were performed for each solvent. The concentration of each solution was determined with a calibration curve in 50:50 methanol/water using different concentrations, viz., 5, 10, 20, 40, 80, 120, and 200 μg/mL.

Determination of the Partition Coefficient. The log P value was determined by the miniaturized shake flask method.[28] Stock solutions (200 μL) of KRM-II-81 and the KRM-II-81·HCl salt (1000 μg/mL prepared in *n*-octanol) were taken in Eppendorf tubes. Upon addition of 300 μL of presaturated *n*-octanol and 500 μL of presaturated water, the volume was made up to 1 mL. Eppendorf tubes were shaken overnight at 500 rpm and centrifuged at 16 000 RCF (*G*-force) for 20 min to separate aqueous and organic layers. Three aliquots of 10 μL of the octanol layer were combined with 70 μL of octanol, and this was followed by the determination of absorbance at 300 nm using a 384-well plate (Coring UV star) and a Tecan M1000 microplate reader. The absorbance of the water layer was determined at 300 nm using a 384-well plate (Coring UV star) and the Tecan M1000. Calibration curves for octanol and water were prepared to determine the concentrations of the free base and also the salt. The assays were carried out in triplicate.

pH−Solubility Profile of the KRM-II-81·HCl Salt. The solubility of the KRM-II-81·HCl salt was determined at different pH (pH 1−9) values, according to the procedure that is described above. The following buffers were used and adjusted with KCl to an ionic strength of 0.1 M: pH 9, 8, 7, 6, 5, 4, and 3, 50 mM phosphate buffer; pH 1 and 2, 40 mM HCl acid buffer.

Hygroscopicity Determination. The hygroscopicity of the KRM-II-81·HCl salt was determined at 25 °C at a relative humidity of 80% for 24 h; 0.5 g of KRM-II-81·HCl salt was weighed within an accuracy of 0.01 mg of the salt. The powder was then evenly spread on a watch glass by gently tapping. The salt was then placed on the benchtop, exposing it to 79.5% relative humidity (RH). The increase in weight was checked every 20 min up to 4−5 h. After showing a maximum increase in weight, it was followed by a slight decrease and reached a steady-state level. The analysis was continued for up to 24 h and stopped when the maximum weight was reached.

Kinetic Solubility Assessment. The solubility of KRM-II-81·HCl and its free base was also investigated over a period of 2 h. All studies were performed using a 384-well plate (Corning UV star) and the Tecan M1000, as described earlier. The time-dependent solubility profile of the KRM-II-81·HCl salt and the free base form was measured in water at 37 °C. An excess of the KRM-II-81·HCl salt and KRM-II-81 was added to 10 mL of water under shaking at 300 rpm. An aliquot of 1 mL was taken out at 10, 20, 40, 60, 80, 90, and 120 min. The samples were filtrated through a 0.45 μm poly(vinyl difluoride) (PVDF)

https://doi.org/10.1021/acsomega.2c03029
ACS Omega 2022, 7, 27550−27559

syringe filter, diluted with methanol, and analyzed on a 384-well plate (Coring UV star) on the Tecan M1000 to determine the solubility. Calibration curves for water were prepared to determine the concentrations of the free base and salt. The assays were carried out in triplicate.

In Vivo Studies. Compounds, KRM-II-81 and its HCl salt, were synthesized by the Milwaukee group as previously described.[3,9,29] The other compounds were obtained from Sigma-Aldrich (St. Louis, Missouri).

Rodent Assays. The guidelines of the national government and by the local animal care and use committees were followed when performing all studies. The local animal care and use committee and veterinary staff provided a direct oversight of the animals by inspections, protocol reviews, laboratory site visits, and animal health monitoring at the University of Serbia and St. Vincent Hospital, Indianapolis, IN.

Oral Dose Pharmacokinetics. *Animals.* To determine pharmacokinetic parameters and concentration−time profiles of the selected ligands, we performed a standard pharmacokinetic study in adult male Sprague−Dawley rats bred in the vivarium of the Faculty of Pharmacy, Belgrade, Serbia. The animals were divided into five groups, and they were maintained under standard laboratory conditions (21 ± 2 °C, relative humidity of 40−45%, and illumination of 120 lx) with free access to pellet food and tap water. The rats were kept in 12:12 h light/dark cycle with lights on at 06.00 h, and all handling and testing took place during the light phase of the diurnal cycle.

The study was conducted within the project approved by the Ethical Council for the Protection of Experimental Animals of the Ministry of Agriculture, Forestry, and Water Management of the Republic of Serbia.

Pharmacokinetic Study. To determine pharmacokinetic parameters after oral gavage and obtain the respective pharmacokinetic profiles using the cassette method, the compounds were divided into three cohorts of five groups of animals; each group contained three animals and corresponded to predetermined time intervals (15 min, 40 min, 2 h, 6 h, and 24 h). The first cassette was composed of KPP-IV-09, KPP-III-51, and KRM-II-81, and the second cassette was composed of KPP-III-34, ZK-III-58, and KRM-II-81·HCl. All ligands were given at a dose of 2.0 mg/kg (0.4 mg/mL concentration in 0.25% methyl cellulose in distilled water).

The animals were anesthetized by the intraperitoneal administration of ketamine hydrochloride (90 mg/kg, Ketamidor, Richter Pharma AG, Wels, Austria) and xylazine hydrochloride (10 mg/kg, Xylased, Bioveta, A. S., Ivanovice na Hane, Czech Republic), and the samples of blood (collected via cardiac puncture with heparinized syringes) and brains were taken at the appropriate time intervals. Plasma was obtained after centrifugation for 10 min at 1000*g* (MiniSpin plus centrifuge, Eppendorf, Germany). Brain tissue samples were weighed and homogenized in 1 mL of methanol via an ultrasonic probe (70% amplitude 2 × 20 s). Supernatants were separated after centrifugation for 20 min at 3400*g* (MiniSpin plus centrifuge, Eppendorf, Germany). The plasma and supernatants that were obtained were further processed with solid-phase extraction using Oasis HLB cartridges (Waters Corporation, Milford, Massachusetts). The procedure of sample preparation and determination of concentration was carried out by ultra-performance liquid chromatography−tandem mass spectrometry (UPLC−MS/MS) with a Thermo Scientific Accela 600 UPLC system connected to a Thermo Scientific TSQ Quantum Access MAX triple quadrupole mass spectrometer (Thermo Fisher Scientific, San Jose, California). It was equipped with an electrospray ionization (ESI) source and has already been described in detail.[30] Noncompartmental pharmacokinetic analysis was performed using PK functions for Microsoft Excel software (by Joel Usansky, Atul Desai, and Diane Tang-Liuwere, Department of Pharmacokinetics and Drug Metabolism, Allergan, Irvine, California; https://www.pharmpk.com/soft.html), while graphs were constructed using commercial statistical software Sigma Plot 12 (Systat Software Inc.).

Oral Dose: PTZ Seizures. *PTZ Seizures.* The PTZ seizures were evaluated in male C57BL/6N mice (Charles River, Indianapolis, IN). The potential anticonvulsants were dissolved in 1% carboxymethylcellulose, and pentylenetetrazole (PTZ) was dissolved in 0.9% NaCl. The compounds were dosed at 10 mL/kg. The mice were returned to their home cages for the pretreatment period after administering the test compound by oral gavage. They were then given PTZ by s.c. injection at 70 mg/kg. The latency to produce clonic seizures and the latency to produce tonic seizures were measured using a stopwatch to the second by a trained observer. Time to death was also measured over a 60 min observation period.

Latency to clonus and tonus was analyzed separately by one-way ANOVA, and this was followed by Tukey's test with a priori probabilities of 0.05 being required for rejection of the null hypothesis. Lethality of mice was observed over a 60 min observation period after PTZ, and the latency to death was recorded. The number of mice that died in the PTZ-alone group (vehicle + 70 mg/kg PTZ) was compared to each compound dose by Fisher's Exact Probability test, with $p < 0.05$ being set as the a priori level needed for defining a statistically significant difference.

■ ASSOCIATED CONTENT

Supporting Information

The Supporting Information is available free of charge at https://pubs.acs.org/doi/10.1021/acsomega.2c03029.

^{1}H NMR and ^{13}C NMR spectra of compounds; difference in chemical shift observed between the number of protons of KRM-II-81 and its HCl salt; X-ray crystal data and structure refinement for the KRM-II-81·HCl salt; and physical characteristics (solubility, hygroscopicity, and kinetic solubility) of the KRM-II-81·HCl salt and its free base (PDF)

■ AUTHOR INFORMATION

Corresponding Author

Md Yeunus Mian − *Department of Chemistry and Biochemistry, Milwaukee Institute of Drug Discovery, University of Wisconsin-Milwaukee, Milwaukee, Wisconsin 53211, United States;* orcid.org/0000-0002-7520-1750; Phone: +414-937-0347; Email: mmian@uwm.edu

Authors

Branka Divović − *Department of Pharmacology, Faculty of Pharmacy, University of Belgrade, Belgrade 11000, Serbia*

Dishary Sharmin − *Department of Chemistry and Biochemistry, Milwaukee Institute of Drug Discovery, University of Wisconsin-Milwaukee, Milwaukee, Wisconsin 53211, United States*

Kamal P. Pandey − *Department of Chemistry and Biochemistry, Milwaukee Institute of Drug Discovery, University of*

https://doi.org/10.1021/acsomega.2c03029
ACS Omega 2022, 7, 27550−27559

Wisconsin-Milwaukee, Milwaukee, Wisconsin 53211, United States; orcid.org/0000-0002-0723-2264

Lalit K. Golani − *Department of Chemistry and Biochemistry, Milwaukee Institute of Drug Discovery, University of Wisconsin-Milwaukee, Milwaukee, Wisconsin 53211, United States*

V. V. N. Phani Babu Tiruveedhula − *Department of Chemistry and Biochemistry, Milwaukee Institute of Drug Discovery, University of Wisconsin-Milwaukee, Milwaukee, Wisconsin 53211, United States*

Rok Cerne − *Laboratory of Antiepileptic Drug Discovery, St. Vincent's Hospital, Indianapolis, Indiana 46260, United States; Department of Anatomy and Cell Biology, Indiana University/Purdue University, Indianapolis, Indiana 46202, United States; Faculty of Medicine, University of Ljubljana, 1000 Ljubljana, Slovenia; RespireRx Pharmaceuticals Inc., Glen Rock, New Jersey 07452, United States*

Jodi L. Smith − *Laboratory of Antiepileptic Drug Discovery, St. Vincent's Hospital, Indianapolis, Indiana 46260, United States*

Xingjie Ping − *Department of Anatomy and Cell Biology, Indiana University/Purdue University, Indianapolis, Indiana 46202, United States*

Xiaoming Jin − *Department of Anatomy and Cell Biology, Indiana University/Purdue University, Indianapolis, Indiana 46202, United States*

Gregory H. Imler − *Naval Research Laboratory, Washington, District of Columbia 20375, United States;* orcid.org/0000-0002-9686-9186

Jeffrey R. Deschamps − *Naval Research Laboratory, Washington, District of Columbia 20375, United States*

Arnold Lippa − *RespireRx Pharmaceuticals Inc., Glen Rock, New Jersey 07452, United States*

James M. Cook − *Department of Chemistry and Biochemistry, Milwaukee Institute of Drug Discovery, University of Wisconsin-Milwaukee, Milwaukee, Wisconsin 53211, United States; RespireRx Pharmaceuticals Inc., Glen Rock, New Jersey 07452, United States;* orcid.org/0000-0001-5512-3022

Miroslav M. Savić − *Department of Pharmacology, Faculty of Pharmacy, University of Belgrade, Belgrade 11000, Serbia;* orcid.org/0000-0002-6934-9193

James Rowlett − *Department of Psychiatry and Human Behavior, University of Mississippi Medical Center, Jackson, Mississippi 39216, United States*

Jeffrey M. Witkin − *Department of Chemistry and Biochemistry, Milwaukee Institute of Drug Discovery, University of Wisconsin-Milwaukee, Milwaukee, Wisconsin 53211, United States; Laboratory of Antiepileptic Drug Discovery, St. Vincent's Hospital, Indianapolis, Indiana 46260, United States; RespireRx Pharmaceuticals Inc., Glen Rock, New Jersey 07452, United States*

Complete contact information is available at: https://pubs.acs.org/10.1021/acsomega.2c03029

Author Contributions

All authors participated in research design and conceptualization. M.Y.M., B.D., D.S., K.P.P., X.P., and G.H.I. conducted experiments; M.Y.M., B.D., D.S., and K.P.P. contributed new reagents or analytic tools; data analysis was performed by all authors; and the manuscript was written or contributed by all authors.

Notes

The authors declare no competing financial interest.

J.M.W. has affiliation with the abovementioned institutions along with Witkin consulting, Neuroscience and Trauma Research, which is in the ACS paragon plus system.

■ ACKNOWLEDGMENTS

The authors are grateful to John and Nancy Peterson for their support of this research. The authors thank the following granting agencies for support: DA011792, DA-043204, and NS-076517 and the National Science Foundation, Division of Chemistry [Grant CHE-1625735]. They also acknowledge the UW-Milwaukee Shimadzu Laboratory for Advanced and Applied Analytical Chemistry and support from the Milwaukee Institute of Drug Discovery and the University of Wisconsin-Milwaukee Research Foundation. The authors thank the Office of Naval Research (Award No. N00014-15-WX-0-0149). Part of this work was funded by the Ministry of Education, Science, and Technological Development, Republic of Serbia, through Grant Agreement with University of Belgrade-Faculty of Pharmacy No: 451-03-9/2021-14/200161.

■ REFERENCES

(1) Cerne, R.; Lippa, A.; Poe, M. M.; Smith, J. L.; Jin, X.; Ping, X.; Golani, L. K.; Cook, J. M.; Witkin, J. M. GABAkines − Advances in the Discovery, Development, and Commercialization of Positive Allosteric Modulators of GABAA Receptors. *Pharmacol. Ther.* **2021**, No. 108035.

(2) Witkin, J. M.; Lippa, A.; Smith, J. L.; Jin, X.; Ping, X.; Biggerstaff, A.; Kivell, B. M.; Knutson, D. E.; Sharmin, D.; Pandey, K. P.; Mian, M. Y.; Cook, J. M.; Cerne, R. The Imidazodiazepine, KRM-II-81: An Example of a Newly Emerging Generation of GABAkines for Neurological and Psychiatric Disorders. *Pharmacol. Biochem. Behav.* **2022**, *213*, No. 173321.

(3) Poe, M. M.; Methuku, K.; Li, G.; Verma, A.; Teske, K.; Stafford, D.; Arnold, L. A.; Cramer, J.; Jones, T.; Cerne, R.; Krambis, M.; Witkin, J.; Jambrina, E.; Rehman, S.; Ernst, M.; Cook, J. M.; Schkeryantz, M. M. Synthesis and Characterization of a Novel γ-Aminobutyric Acid Type A ($GABA_A$) Receptor Ligand That Combines Outstanding Metabolic Stability, Pharmacokinetics, and Anxiolytic Efficacy. *J. Med. Chem.* **2016**, *59*, 10800−10806.

(4) Witkin, J. M.; Cerne, R.; Wakulchik; M, J. S.; Gleason, S. D.; Jones, T. M.; Li, G.; Arnold, L. A.; Li, J. X.; Schkeryantz, J. M.; Methuku, K. R.; Cook, J. M.; Poe, M. M. Further Evaluation of the Potential Anxiolytic Activity of Imidazo[1,5-a][1,4]diazepin Agents Selective for α2/3-containing GABAA Receptors. *Pharmacol. Biochem. Behav.* **2017**, *157*, 35−40.

(5) Methuku, K. R.; Li, X.; Cerne, R.; Gleason, S.; Schkeryantz, J. M.; Tiruveedhula, V. V. N.; Golani, L. K.; Li, G.; Poe, M.; Rahman, M. T.; Cook, J.; Fisher, J.; Witkin, J. An Antidepressant-Related Pharmacological Signature for Positive Allosteric Modulators of alpha 2/3-Containing GABAA Receptors. *Pharmacol. Biochem. Behav.* **2018**, *170*, 9−13.

(6) Witkin, J. M.; Cerne, R.; Davis, P. G.; Freeman, K. B.; DoCarmo, J. M.; Rowlett, J. K.; Methuku, K. R.; Okun, A.; Gleason, S. D.; Li, X.; Krambis, M. J.; Poe, M.; Li, G.; Schkeryantz, J. M.; Jahan, R.; Yang, L.; Guo, W.; Golani, L. K.; Anderson, W. H.; Catlow, J. T.; Jones, T. M.; Porreca, F.; Smith, J. L.; Knopp, K. L.; Cook, J. M. The α2,3-Selective Potentiator of GABAA Receptors, KRM-II-81, Reduces Nociceptive-Associated Behaviors Induced by Formalin and Spinal Nerve Ligation in Rats. *Pharmacol. Biochem. Behav.* **2019**, *180*, 22−31.

(7) Witkin, J. M.; Smith, J. L.; Ping, X.; Gleason, S. D.; Poe, M. M.; Li, G.; Jin, X.; Hobbs, J.; Schkeryantz, J. M.; McDermott, J. S.; Alatorre, A. I.; Siemian, J. N.; Cramer, J. W.; Airey, D. C.; Methuku, K. R.; Tiruveedhula, V. V. N. P. B.; Jones, T. M.; Crawford, J.; Rambis, M. J.; Fisher, J. L.; Cook, J. M.; Cerne, R. Bioisosteres of Ethyl 8-ethynyl-6-(pyridin-2-yl)-4H-benzo[f]imidazo [1,5-a][1,4]diazepine-3-carboxylate (HZ-166) as Novel Alpha 2,3 Selective Potentiators of GABAA

Receptors: Improved Bioavailability Enhances Anticonvulsant Efficacy. *Neuropharmacology* **2018**, *137*, 332−343.
(8) Witkin, J. M.; Ping, X.; Cerne, R.; Mouser, C.; Jin, X.; Hobbs, J.; Tiruveedhula, V.V.N.; Li, G.; Jahan, R.; Rashid, F.; Kumar, G. L.; Cook, J. M.; Smith, J. L. The Value of Human Epileptic Tissue in the Characterization and Development of Novel Antiepileptic Drugs: The example of CERC-611 and KRM-II-81. *Brain Res.* **2019**, *1722*, No. 146356.
(9) Knutson, D. E.; Jodi, L. M.; Ping, X.; Jin, X.; Golani, L. K.; Li, G.; Tiruveedhula, V. V. N.; Rashid, R.; Mian, M. D.; Jahan, R.; Sharmin, D.; Cerne, R.; Cook, J. M.; Witkin, J. M. Imidazodiazepine Anticonvulsant, KRM-II-81, Produces Novel, Non-diazepam-like Antiseizure Effects. *ACS Chem. Neurosci.* **2020**, *11*, 2624−2637.
(10) Cerne, R.; Smith, J. L.; Fisher, J. L.; Golani, L. K.; Knutson, D. E.; Cook, J. M.; Witkin, J. M.The Orally Bioavailable Imidazodiazepine, KRM-II-81, is a Novel Potentiator of α2/3-Containing GABAA Receptors with Analgesic Efficacy. In *The Neurobiology, Physiology, and Psychology of Pain*; Rajendram, R.; Patel, V. B.; Preedy, V. R.; Martin, C. R., Eds.; Academic Press, 2022; Chapter 11, pp 117−127.
(11) Biggerstaff, A.; Kivell, B.; Smith, J. L.; Mian, M. D.; Golani, L. K.; Rashid, F.; Sharmin, D.; Knutson, D. E.; Cerne, R.; Cook, J. M.; Witkin, J. M. The α2,3-selective Potentiators of GABAA Receptors, KRM-II-81 and MP-III-80, Produce Anxiolytic-like Effects and Block Chemotherapy-induced Hyperalgesia in Mice without Tolerance Development. *Pharmacol. Biochem. Behav.* **2020**, *196*, No. 172996.
(12) Gardner, C. R.; Walsh, C. T.; Almarsson, O. Drugs as Materials: Valuing Physical Form in Drug Discovery. *Nat. Rev. Drug Discovery* **2004**, *3*, 926−934.
(13) Lipinski, C. Poor Aqueous Solubility-An Industry Wide Problem in Drug Discovery. *Am. Pharm. Rev.* **2002**, *5*, 82−85.
(14) Serajuddin, A. T. Salt Formation to Improve Drug Solubility. *Adv. Drug Delivery Rev.* **2007**, *59*, 603−616.
(15) Hawley, M.; Morozowich, W. Modifying the Diffusion Layer of Soluble Salts of Poorly Soluble Basic Drugs to Improve Dissolution Performance. *Mol. Pharm.* **2010**, *7*, 1441−1449.
(16) Paulekuhn, G. S.; Dressman, J. B.; Saal, C. Salt Screening and Characterization for Poorly Soluble, Weak Basic Compounds: Case Study Albendazole. *Pharmazie* **2013**, *68*, 555−556.
(17) Mukesh, S.; Joshi, P.; Bansal, A. K.; Kashyap, M. C.; Mandal, S. K.; Sathe, V.; Sangamwar, A. T. Amorphous Salts Solid Dispersions of Celecoxib: Enhanced Biopharmaceutical Performance and Physical Stability. *Mol. Pharm.* **2021**, *18*, 2334−2348.
(18) Kumar, V.; Bharate, S. B.; Vishwakarma, R. A.; Bharate, S. S. Selection of a Water-Soluble Salt Form of a Preclinical Candidate, IIIM-290: Multiwell-Plate Salt Screening and Characterization. *ACS Omega* **2018**, *3*, 8365−8377.
(19) Sareen, S.; George, M.; Lincy, J. Improvement in Solubility of Poor Water-soluble Drugs by Solid Dispersion. *Int. J. Pharm. Invest.* **2012**, *2*, 12−17.
(20) Cumming, H.; Rucker, C. Octanol−Water Partition Coefficient Measurement by a Simple ^{1}H NMR Method. *ACS Omega* **2017**, *2*, 6244−6249.
(21) Andersin, R. Solubility and Acid-Base Behaviour of Midazolam in Media of Different pH, Studied by Ultraviolet Spectrophotometry with Multicomponent Software. *J. Pharm. Biomed. Anal.* **1991**, *9*, 451−455.
(22) Bruker *APEX3*, v2019.1-0; Bruker AXS Inc.: Madison, Wisconsin, USA, 2019.
(23) Bruker *SAINT*, v8.38A; Bruker AXS Inc.: Madison, Wisconsin, USA, 2017.
(24) Bruker *XPREP*, v2014/2; Bruker AXS Inc.: Madison, Wisconsin, USA, 2014.
(25) Bruker *SADABS*, v2016/2; Bruker AXS Inc.: Madison, Wisconsin, USA, 2016.
(26) Bruker *SHELXTL*, v2018/3; Bruker AXS Inc.: Madison, Wisconsin, USA, 2018.
(27) Bharate, S. S.; Vishwakarma, R. A. Thermodynamic Equilibrium Solubility Measurements in Simulated Fluids by 96-well Plate Method in Early Drug Discovery. *Bioorg. Med. Chem. Lett.* **2015**, *25*, 1561−1567.
(28) Kumar, V.; Bharate, S. S.; Vishwakarma, R. A. Modulating Lipophilicity of Rohitukine via Prodrug Approach: Preparation, Characterization, and in Vitro Enzymatic Hydrolysis in biorelevant media. *Eur. J. Pharm. Sci.* **2016**, *92*, 203−211.
(29) Pandey, K. P.; Khan, M. Z. A.; Golani, L. K.; Mondal, P.; Mian, M. Y.; Rashid, F.; Tiruveedhula, V. V. N. P. B.; Knutson, D. E.; Sharmin, D.; Ahmed, T.; Rezvanian, S.; Zahn, N. M.; Arnold, L. A.; Witkin, J. F.; Cook, J. M. Design, Synthesis and Characterization of Novel Gamma Aminobutyric Acid type A Receptor Ligands. *ARKIVOC* **2021**, *2020*, 242−256.
(30) Obradović, A. L.; Joksimović, S.; Poe, M. M.; Ramerstorfer, J.; Varagic, Z.; Namjoshi, O.; Batinić, B.; Radulović, T.; Marković, B.; Roth, B. L.; Sieghart, W.; Cook, J. M.; Savić, M. M. Sh-I-048A, an in Vitro Non-selective Super-agonist at the Benzodiazepine Site of GABAA Receptors: The Approximated Activation of Receptor Subtypes May Explain Behavioral Effects. *Brain Res.* **2014**, *1554*, 36−48.

https://doi.org/10.1021/acsomega.2c03029
ACS Omega 2022, 7, 27550−27559